

# Spectral distribution of the two-photon decay of He-like krypton

R. Ali <sup>a,\*</sup>, I. Ahmad <sup>a</sup>, H.G. Berry <sup>a</sup>, R.W. Dunford <sup>a</sup>, D.S. Gemmell <sup>a</sup>, E.P. Kanter <sup>a</sup>,  
 P.H. Mokler <sup>b</sup>, A.E. Livingston <sup>c</sup>, S. Cheng <sup>d</sup>, L.J. Curtis <sup>d</sup>

<sup>a</sup> *Physics Division, Argonne National Laboratory, Argonne, IL 60439, USA*

<sup>b</sup> *GSI Darmstadt, Darmstadt, Germany*

<sup>c</sup> *Department of Physics, University of Notre Dame, Notre Dame, IN 46556, USA*

<sup>d</sup> *Department of Physics and Astronomy, University of Toledo, Toledo, OH 43606, USA*

## Abstract

We report progress on a measurement of the spectral distribution of photons from the two-photon decay of the  $2^1S_0$  level in heliumlike krypton. A measurement of the exact shape of the continuum singles spectrum of the two-photon decay in heliumlike ions provides a sensitive probe of the calculation of the transition probability. In our experiment, a beam of  $Kr^{34+}$  ions is excited using a thin carbon foil and the subsequent decays are observed in an array of four X-ray detectors.

## 1. Introduction

The  $2^1S_0$  state in heliumlike ions is forbidden to decay to the ground state by the emission of a single photon so the dominant decay mode is emission of two E1 photons. The energies of the individual photons have a continuous distribution with a broad peak at half the transition energy and the sum of the energies of the two photons is equal to the transition energy. Calculations of the two-photon decay rate and the spectral distribution have been done by Dalgarno et al. [1,2], Victor et al. [3,4], Jacobs [5], and Drake [6]. Electron correlations give rise to a dependence of the spectral shape on the nuclear charge. A comparison of the spectral shape for He and He-like Kr is given in Fig. 1(a).

The relativistic corrections to the spectral shape have not been calculated for He-like systems, however fully relativistic calculations for the H-like decay have been done by Parpia and Johnson [7,8] and by Goldman and Drake [9,10]. A comparison of the spectral shapes for the decay of the  $2^2S_{1/2}$  level in H-like ions is presented in Fig. 1(b) for  $Z = 1$  and  $Z = 40$ . This shows that the relativistic effects also lead to a dependence of the shape on nuclear charge.

The two-photon decay rate in He-like ions has been measured to a precision of about 1% in  $Kr^{34+}$  [11],  $Br^{35+}$  [12], and  $Ni^{26+}$  [13]; and to lower precision in  $Nb^{39+}$  [14],  $Ar^{16+}$  [15],  $Li^+$  [16], and helium [17,18]. To date, no detailed measurement of the spectral shape has been made at any  $Z$ . The goal of our experiment is to make a

precision measurement of the spectral shape of the decay of the  $2^1S_0$  level in He-like krypton in order to test the nonrelativistic calculations of Drake as well as provide sensitivity to the relativistic corrections.

## 2. Experiment

The experiment utilized an 805-MeV beam of  $^{84}Kr$  ions provided by the Argonne Tandem-Linac (ATLAS). The beam came in bunches separated by 82.5 ns which were about 1 ns wide at our target position. After the beam was stripped in a  $200\text{-}\mu\text{g}/\text{cm}^2$  carbon foil the  $34+$  charge state was magnetically selected and directed to our target chamber. In the chamber, the ions were excited by a  $10\text{-}\mu\text{g}/\text{cm}^2$  carbon foil. The region of the beam downstream of the foil was viewed by an array of four X-ray detectors. The array consisted of three Si(Li) detectors and a five-fold Ge detector. A "shield" consisting of a thin molybdenum sheet with a 6-mm diameter aperture was placed upstream of the target. This shield, together with molybdenum collimators placed over each detector, prevented X-rays coming directly from the target from being detected. This eliminated the intense radiation from short-lived states. The foil holder was mounted on a translation stage which allowed accurate positioning relative to the detectors. After determination of the optimum location for the foil, its position was kept fixed for the remainder of the experiment.

A typical spectrum for one of the Si(Li) detectors is given in Fig. 2. The peak at 13 keV is from single-photon decays of the  $n = 2$  states of He-like krypton and is

\* Corresponding author.

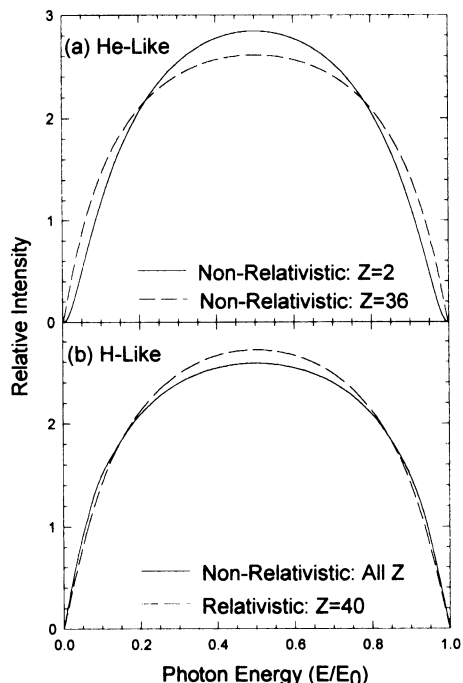


Fig. 1. Photon energy distributions for the two-photon decays of the H-like  $2^2S_{1/2}$  state (top) and He-like  $2^1S_0$  state (bottom).  $E/E_0$  is the fraction of the energy relative to the transition energy  $E_0$ .

dominated by the M1 decay of the  $2^3S_1$  level. The continuum on the low energy side of this peak has contributions from two-photon decay of the  $2^1S_0$  level in heliumlike krypton, but other processes such as H-like two-photon decays, X-ray scattering, fluorescence, and incomplete charge collection in the Si(Li) detector contribute. The other prominent features in the spectrum include decays into  $n=2$  which contribute X-rays in the region below 4.5 keV and characteristic X-rays from fluorescence of the collimators (molybdenum) or other materials in the chamber. It is clear that it is not possible to make a reliable measurement of the spectral shape for two-photon decay from the singles spectrum.

Most of the data were taken with a  $10\text{-}\mu\text{g}/\text{cm}^2$  thick carbon foil, although we took some data with an  $80\text{-}\mu\text{g}/\text{cm}^2$  thick carbon foil as a check on systematic effects. The foil thickness was chosen to optimize the production of the  $2^1S_0$  level while minimizing population of other levels which contribute to unwanted backgrounds. In earlier work [12,19] we found that thin foils gave a higher yield for the  $2^1S_0$  level relative to the yield for other heliumlike states.

Standard coincidence electronics were used for data collection. The preamp outputs on the detectors were sent to both fast and slow amplifiers to give timing and energy signals for each detector. Shaping times of 0.25 and  $2\ \mu\text{s}$  were used for the fast and slow amplifiers, respectively.

The electronic efficiency was determined by simultaneously recording X-ray and pulser spectra. The intensity of the pulser peak relative to that of the X-ray lines was determined for energies down to 0.7 keV, thus yielding the electronic efficiency curves. By means of fast/slow timing coincidence, it was possible to set the threshold low enough to obtain a unity electronic efficiency down to 1.2 keV for the three Si(Li) detectors.

If two photons were incident on a detector within the integration time of the slow amplifier, a ‘‘pileup’’ occurred and the energy measurement for that event was incorrect. To eliminate this, any event in which two timing signals were received for the same detector within  $20\ \mu\text{s}$  was tagged as a pileup event and these were rejected in the data analysis.

Fig. 3 shows the correlation between the energies for Dets. A and B for coincident events. The two-photon decays form a diagonal line corresponding to events with the same sum energy  $E_0 = E_A + E_B$ , where  $E_0$  is the transition energy and  $E_A$  and  $E_B$  are the energies of the individual photons. The other features in the figure are caused by accidental coincidences. Fig. 4 is a time-difference spectrum for coincidences between detectors A and B. The prominent peak in the center is due to events originating from the same beam pulse. Random coincidences that appear to either side exhibit the beam pulse structure of the LINAC. The random coincidence rate can be reliably determined by analyzing the events in the shaded windows. These windows are symmetric with respect to the beam pulse structure.

### 3. Results

Partial data analysis has been completed for coincidences between two of the Si(Li) detectors used in the

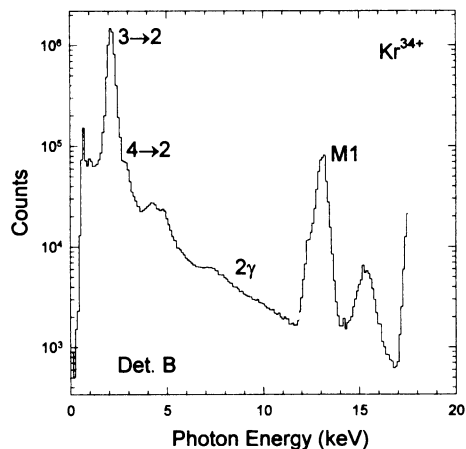


Fig. 2. Singles spectrum for detector B. The energies of the lines are broadened and shifted by the Doppler effect.

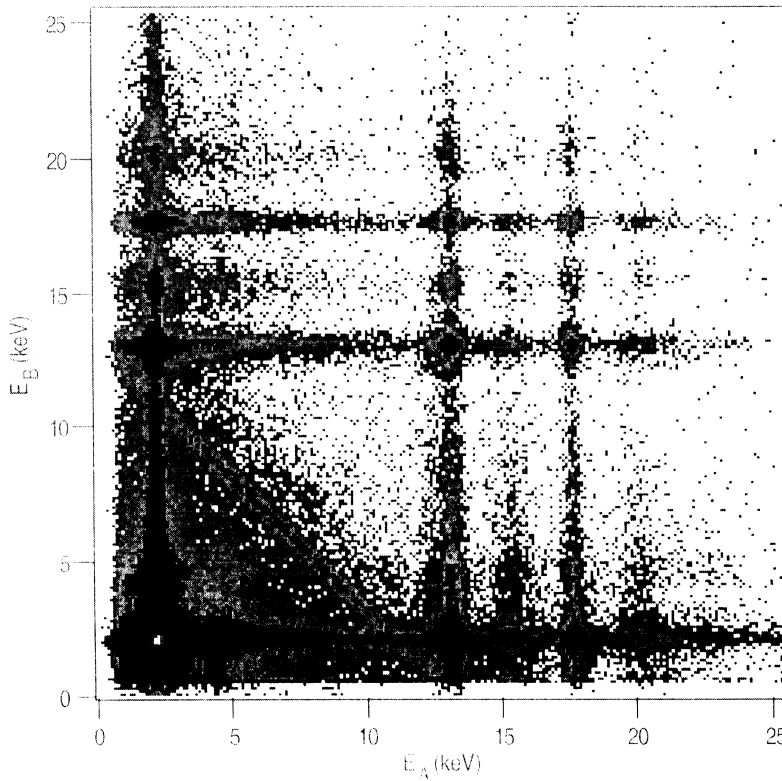


Fig. 3. Two-dimensional scatter plot for coincidence events in detectors A and B. The diagonal line represents the two-photon decays.

experiment (Det. A and Det. B). These detectors lie along a line perpendicular to the beam axis, facing each other. Fig. 5 is a sum-energy spectrum formed by adding the energies from detectors A and B for each coincidence event. The two-photon events are in the peak at a sum-en-

ergy of 13 keV. The other peak comes from accidental coincidences. In Fig. 6(a), we show a spectrum measured by Det. B for events which are in both the two-photon peak of the sum-energy spectrum and the random window of the time-difference spectrum (see Fig. 4). Fig. 6(b)

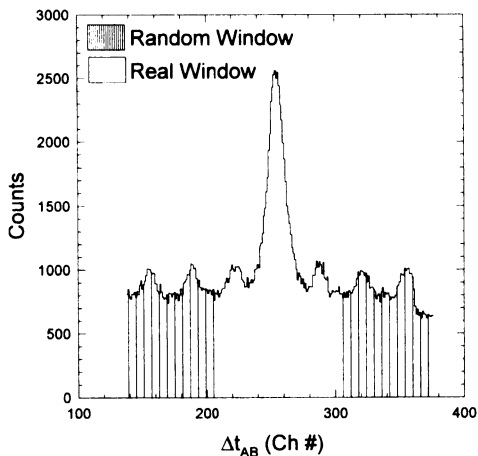


Fig. 4. Time-difference spectrum for coincidence events in detectors A and B. The windows shown are used to obtain spectra corresponding to real and random coincidences.

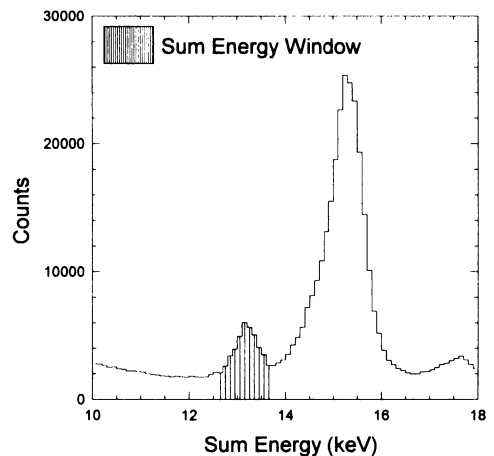


Fig. 5. Sum-energy spectrum for detectors A and B. The shaded region corresponds to the proper sum-energy for the two-photon decay of the  $2^1S_0$  level in He-like Kr.

shows the same spectrum except that the events are from the real window of the time-difference spectrum. If these two spectra are subtracted from each other, after suitable weighting for the widths of the cuts in the time-difference spectra, the result should be the raw two-photon spectral shape. These data would then need to be corrected for overall coincidence detection efficiency in order to obtain the corrected spectral shape to be compared with theory. However, we have found that the subtraction procedure does not result in a purely two-photon spectrum because there are additional true coincidences from cascade events which contribute to the true coincidences of Fig. 6(b). There are also some true coincidences arising from interaction of the beam with the shield which are not eliminated by a simple subtraction of randoms. A more complicated analysis is required to eliminate these additional spurious events and this work is still in progress.

Several considerations are involved in the determination of the coincidence efficiency in our experiment. We must characterize both the intrinsic detector efficiency and the efficiency of the acquisition electronics as a function of photon energy. In addition, we must take into account such details as the beam velocity, the decay distribution of beam ions, the angular distribution of decay radiation and the detailed geometry of our detectors. In order to properly account for all of these factors, we have developed a

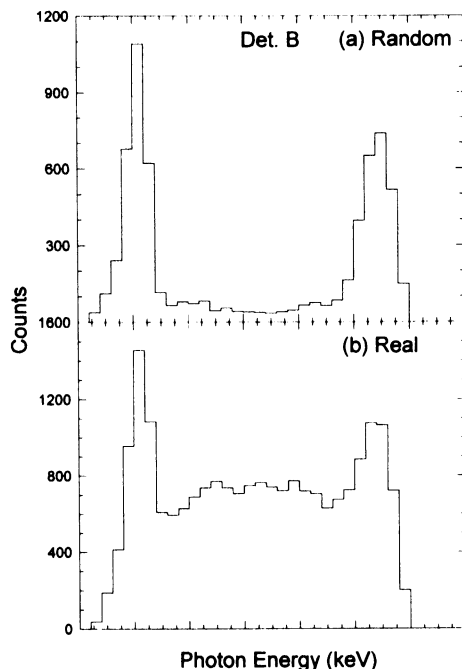


Fig. 6. Spectra in detector B corresponding to the random (a) and real (b) windows in Fig. 4. We also require the proper sum-energy for two-photon decay (see Fig. 5).

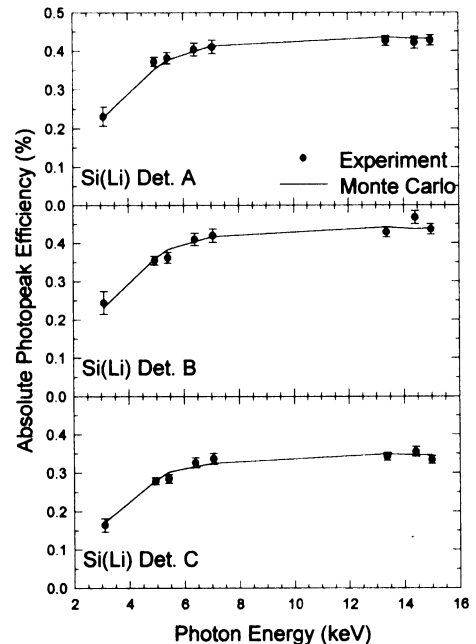


Fig. 7. Absolute experimental and Monte Carlo simulation photopeak efficiencies for detectors A, B, and C. The Monte Carlo simulation takes into account the beryllium, gold, and silicon dead layer frontal absorbers as well as the geometry of the detectors.

Monte Carlo simulation program to model our experiment. To provide precise information for inclusion in the code, careful measurements were made of the geometry of the foil holders, collimators and detector crystals. The intrinsic efficiencies of the detectors were determined using a set of radioactive sources whose absolute intensities were measured (see Fig. 7). As a test, the Monte Carlo program was used to model the shapes of the 13-keV single-photon line, as well as the lines from the radioactive sources. A comparison of the results from the model and the experiment for the 13-keV M1 line is given in Fig. 8.

#### 4. Conclusion

Our preliminary measurement of the spectral shape of the two-photon decay of He-like krypton demonstrates that the apparatus is sensitive to photon energies down to about 1 keV, and our rate of detection of two-photon events (5 Hz for detectors A and B) is sufficient to provide a detailed comparison of experiment and theory. The Monte Carlo program allows us to account for many details and imperfections in the apparatus and provides a means for detailed comparison with theory. There are some problems which need to be overcome before a reliable comparison with theory can be made. Most importantly, we need a

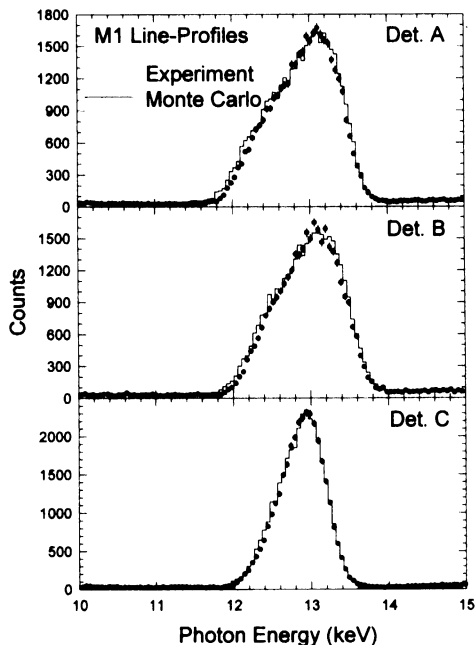


Fig. 8. Experimental and Monte Carlo M1 line-profiles for detectors A, B, and C. The simulation takes into account the Doppler broadening of the lines.

means to eliminate cascade coincidences from our raw spectral shape data. One technique is to recognize that, even though cascades are true coincidences, they do not give rise to a peak in the sum-energy spectrum. We are working on a more complicated data analysis prescription based on this idea. Another difficulty is in the determination of the detector efficiency. This is not adequately determined at present, particularly at the low energy end of the spectrum. We need additional calibration sources to provide better coverage of the entire range of energies down to 1 keV. Finally, we need to eliminate the spurious events arising from the interaction of the beam with the shield.

## Acknowledgements

We thank the staff of ATLAS for providing the Kr beam used in this experiment. We are indebted to Bruce Zabransky and Chuck Kurtz for designing and building the target chamber.

## References

- [1] A. Dalgarno, *Mon. Not. R. Astron. Soc.* 131 (1966) 311.
- [2] A. Dalgarno and G.A. Victor, *Proc. Phys. Soc. London* 87 (1966) 371.
- [3] G.A. Victor, *Proc. Phys. Soc. London* 91 (1967) 825.
- [4] G.A. Victor and A. Dalgarno, *Phys. Rev. Lett.* 18 (1967) 1105.
- [5] V.L. Jacobs, *Phys. Rev. A* 4 (1971) 939.
- [6] G.W.F. Drake, *Phys. Rev. A* 34 (1986) 2871.
- [7] W.R. Johnson, *Phys. Rev. Lett.* 29 (1972) 1123.
- [8] F.A. Parpia and W.R. Johnson, *Phys. Rev. A* 26 (1982) 1142.
- [9] S.P. Goldman and G.W.F. Drake, *Phys. Rev. A* 24 (1981) 183.
- [10] S.P. Goldman, *Phys. Rev. A* 40 (1989) 1185.
- [11] R. Marrus, V.S. Vicente, P. Charles, J.P. Briand, F. Bosch, D. Liesen and I. Varga, *Phys. Rev. Lett.* 56 (1986) 1683.
- [12] R.W. Dunford, H.G. Berry, S. Cheng, E.P. Kanter, C. Kurtz, B.J. Zabransky, A.E. Livingston and L.J. Curtis, *Phys. Rev. A* 48 (1993) 1929.
- [13] R.W. Dunford, M. Hass, E. Bakke, H.G. Berry, C.J. Liu, M.L.A. Raphaelian and L.J. Curtis, *Phys. Rev. Lett.* 62 (1989) 2809.
- [14] A. Simionovici, B.B. Birkett, J.P. Briand, P. Charles, D.D. Dietrich, K. Finlayson, P. Indelicato, D. Liesen and R. Marrus, *Phys. Rev. A* 48 (1993) 1695.
- [15] R. Marrus and R.W. Schmieder, *Phys. Rev. A* 5 (1972) 1160.
- [16] M.H. Prior and H.A. Shugart, *Phys. Rev. Lett.* 27 (1971) 902.
- [17] A.S. Pearl, *Phys. Rev. Lett.* 24 (1970) 703.
- [18] R.S. Van Dyck Jr, C.E. Johnson and H.A. Shugart, *Phys. Rev. A* 4 (1971) 1327.
- [19] R.W. Dunford, H.G. Berry, D.A. Church, M. Hass, C.J. Liu, M.L.A. Raphaelian, B.J. Zabransky, L.J. Curtis and A.E. Livingston, *Phys. Rev. A* 48 (1993) 2729.